JGR Oceans

RESEARCH ARTICLE
10.1029/2024JC021038

Seasonal Variability in Baffin Bay

Xuan Shan[1,2], Michael A. Spall[2], Clark Pennelly[3], and Paul G. Myers[3]

[1]Frontiers Science Center for Deep Ocean Multispheres and Earth System and Key Laboratory of Physical Oceanography, Ocean University of China, Qingdao, China, [2]Woods Hole Oceanographic Institution, Woods Hole, MA, USA, [3]Department of Earth and Atmospheric Sciences, University of Alberta, Edmonton, AB, Canada

Key Points:

- Basin-scale barotropic circulation varies seasonally and is mainly forced by along-topography surface stress
- Baffin Island Current is less surface intensified in ice seasons due to ice-ocean stress curl induced cross-shelf circulation
- Net sea ice formation makes Baffin Bay water densified and increases the sea ice export through Davis Strait

Supporting Information:

Supporting Information may be found in the online version of this article.

Correspondence to:

X. Shan,
xuan.shan@whoi.edu

Citation:

Shan, X., Spall, M. A., Pennelly, C., & Myers, P. G. (2024). Seasonal variability in Baffin Bay. *Journal of Geophysical Research: Oceans*, *129*, e2024JC021038. https://doi.org/10.1029/2024JC021038

Received 12 FEB 2024
Accepted 10 OCT 2024

Author Contributions:

Conceptualization: Xuan Shan, Michael A. Spall
Funding acquisition: Michael A. Spall, Paul G. Myers
Investigation: Xuan Shan
Methodology: Clark Pennelly
Project administration: Michael A. Spall
Resources: Michael A. Spall, Paul G. Myers
Supervision: Michael A. Spall
Visualization: Xuan Shan
Writing – original draft: Xuan Shan
Writing – review & editing: Michael A. Spall, Clark Pennelly, Paul G. Myers

Abstract Three dominant characteristics and underlying dynamics of the seasonal cycle in Baffin Bay are discussed. The study is based on a regional, high-resolution coupled sea ice-ocean numerical model that complements our understanding drawn from observations. Subject to forcing from the atmosphere, sea ice, Greenland, and other ocean basins, the ocean circulation exhibits complex seasonal variations that influence Arctic freshwater storage and export. The basin-scale barotropic circulation is generally stronger (weaker) in summer (winter). The interior recirculation (~2 Sv) is primarily driven by oscillating along-topography surface stress. The volume transport along the Baffin Island coast is also influenced by Arctic inflows (~0.6 Sv) via Smith Sound and Lancaster Sound with maximum (minimum) in June-August (October-December). In addition to the barotropic variation, the Baffin Island Current also has changing vertical structure with the upper-ocean baroclinicity weakened in winter-spring. It is due to a cross-shelf circulation associated with spatially variable ice-ocean stresses that flattens isopycnals. Greenland runoff and sea ice processes dominate buoyancy forcing to Baffin Bay. Opposite to the runoff that freshens the west Greenland shelf, stronger salinification by ice formation compared to freshening by ice melt enables a net densification in the interior of Baffin Bay. Net sea ice formation in the past 30 years contributes to ~25% of sea ice export via Davis Strait. The seasonal variability in baroclinicity and water mass transformation changes in recent decades based on the simulation.

Plain Language Summary Baffin Bay ocean circulation is important for Arctic freshwater exports that may influence subpolar deep convection. However, we have little knowledge about how it works in winter due to limited observations. This study investigates three dominant aspects of the seasonal cycle in Baffin Bay ocean circulation and hydrography with a high-resolution ice-ocean coupled model. The basin-scale barotropic circulation (depth-integrated transport) is stronger in summer and weaker in winter, mainly driven by along-topography surface stress and Arctic inflows. The baroclinicity (vertical velocity shear) of the Baffin Island Current is weakened in winter associated with spatially uneven ice-ocean stresses. Net sea ice formation in Baffin Bay in the past 30 years makes Baffin Bay water densified and increases the sea ice export through Davis Strait. Changes of seasonality in Baffin Bay in the past 30 years are also discussed using model results.

1. Introduction

Baffin Bay is a marginal sea that lies between Greenland and Baffin Island of Canada with the Labrador Sea to the south and the Arctic Ocean to the north (Figure 1). As a connection between the Arctic and subpolar regions, the bay receives warm and salty Atlantic water from the Labrador Sea and fresh and cold polar water from the Canadian Arctic Archipelago (CAA). The latter accounts for about half of the Arctic liquid freshwater discharge (e.g., Haine et al., 2015). Sea ice is exported from the CAA to Baffin Bay as well and melts at lower latitudes. Arctic freshwater discharge through the CAA and Baffin Bay is thought to impact deep convection in the Labrador Sea (e.g., Zhang et al., 2021). Rather than being a passive conduit, Baffin Bay may influence freshwater exports by modifying the ocean velocity field, sea water properties, and the amount of sea ice. Therefore, understanding circulation and water mass transformation in Baffin Bay is important for revealing the freshwater status downstream. It is essential to understand processes in Baffin Bay since more Arctic freshwater discharge is anticipated under global warming (e.g., Haine et al., 2015; Wang et al., 2023).

The horizontal circulation in Baffin Bay has been described with earlier measurements. It is featured by a cyclonic circulation consisting of two boundary current systems (Münchow et al., 2015; Tang et al., 2004). Approximately 3 Sv (1 Sv = 10^6 m^3 s^{-1}) of Atlantic water progresses poleward by the West Greenland Slope Current (~2.5 Sv) over the wide continental slope off Greenland and a coastal current over the Greenland shelf (~0.5 Sv). The currents turn westward around Cape York and merge with approximately 2 Sv Arctic outflows from the northern

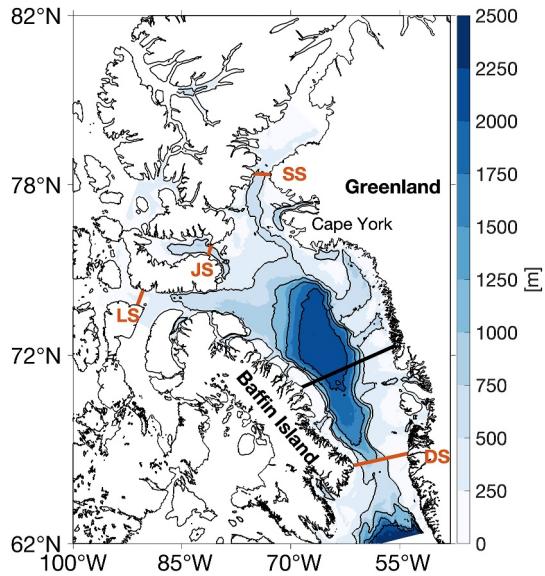

Figure 1. Bathymetry in Baffin Bay and location of straits. The orange lines indicate straits that are defined close to but not exactly along observation arrays (SS for Smith Sound, JS for Jones Sound, LS for Lancaster Sound and DS for Davis Strait). The black line shows a zonal section in the middle of Baffin Bay used to address the seasonality of baroclinic circulation in Figure 5. The 500, 1,000, 1,500 and 2,000 m isobaths are denoted by gray contours. The bathymetry is based on the General Bathymetric Chart of the Oceans (GEBCO) gridded bathymetry data used in our model simulation (Section 2).

channels (Addison, 1987; Muench, 1971): Smith Sound (Münchow, 2016), Lancaster Sound (Peterson et al., 2012) and Jones Sound (Melling et al., 2008). The Atlantic and Arctic waters together form the Baffin Island Current (~5 Sv) that flows equatorward along the narrow continental slope off Canada. The West Greenland Slope Current is bottom intensified and mainly barotropic (Münchow et al., 2015). Meanwhile the Baffin Island Current contains both barotropic and baroclinic components with a larger contribution from the latter (Münchow et al., 2015; Rudels, 2011).

Although the general gyre circulation is documented, it is mostly based on summer observations since conducting scientific cruises in winter is difficult (Fissel et al., 1982; Münchow et al., 2015). The horizontal circulation in Baffin Bay is assumed to exhibit complex seasonal variations under local and remote momentum forcing. Wind patterns over Baffin Bay undergo obvious seasonal changes (Tang et al., 2004). In winter, the wind stress is generally toward south and strong especially in the western Baffin Bay. In summer, the wind stress is mainly toward north and weak (strong) in the western (eastern) Baffin Bay. The efficiency of wind forcing is strongly weakened by sea ice, especially along the Baffin Island coast in winter (Landy et al., 2017). Remote forcing from other oceans also experiences obvious seasonal cycles, especially for volume transports through Lancaster Sound and Davis Strait. The Lancaster Sound volume transport is strong in summer and weak in autumn (Peterson et al., 2012). The Davis Strait transport is stronger in late spring and summer compared to other months (Curry et al., 2014). The volume transports through Smith and Jones Sound show little seasonality (Melling et al., 2008; Münchow, 2016). Each of these seasonal cycles will be discussed in more detail in Section 3.

Water masses transform from one density to another by buoyancy forcing and interior mixing. Baffin Bay receives various buoyancy forcing from the atmosphere, sea ice, and Greenland. The surface heat and freshwater flux are expected to experience strong seasonal variation related to the seasonal cycle of sea ice. According to a previous study (Tang et al., 2004), sea ice reaches its minimum in September and gradually forms from northwest to southeast. It reaches a maximum in April when sea ice covers most of the bay except the eastern side of Davis Strait. Sea ice melts initially in the North Water Polynya and along the Greenland coast, finally to the entire basin. The most remarkable feature of sea ice in Baffin Bay is the continuous ice formation in the North Water Polynya (NOW) in winter accompanied by strong brine rejection, which may be a source of the deep and bottom waters in Baffin Bay (Bourke et al., 1989; Ingram et al., 2002; Melling et al., 2001; Muench, 1971; Yao & Tang, 2003). Sea ice formed in the NOW is advected promptly away from its formation site and carried by the Baffin Island Current, together with sea ice from the northern channels, toward the Labrador Sea. Enhanced Greenland melt goes into Baffin Bay along the coast since the mid-1990s, mainly in summer (Bamber et al., 2018; Grivault et al., 2017).

Seasonal variations in local and remote forcing suggest changes in ocean circulation and hydrography. The winter state may differ from that observed in summer, which has significant implications for Arctic freshwater exports and subpolar deep convection. It motivates us to study the seasonality of the Baffin Bay using a realistic coupled ocean-sea ice model that provides more complete temporal and spatial coverage. The paper is organized as follows: Section 2 describes the numerical experiment and model evaluation. Section 3 analyzes dominant modes of seasonal variability in the Baffin Bay ocean circulation and hydrography: the basin-scale barotropic circulation; the baroclinic circulation; and water mass transformation by buoyancy forcing from the atmosphere, sea ice, and Greenland. Section 4 discusses changes of the seasonal variations in the past 30 years and potential responses to global warming in the future. Section 5 summarizes the findings of our work.

2. Numerical Model Setup and Evaluation

2.1. Model Configuration

In this study, a coupled ocean-sea ice model, the Nucleus for European Modeling of the Ocean (NEMO) version 3.6, is used to conduct the numerical simulation (Madec & the NEMO team, 2008). The ocean is interfaced with an ice model, the Louvain-la-Neuve Ice Model Version 2 (LIM2, Fichefet & Maqueda, 1997; Goosse & Fichefet, 1999). The model domain covers the Arctic and the Northern Hemisphere Atlantic with 1/12° horizontal resolution (ANHA12) as in Hu et al. (2018). The model is eddy permitting with horizontal resolution of about 4 km in Baffin Bay where the local deformation radius is around 9 km. There are 50 geopotential levels with high resolution focused on the upper ocean (22 levels for the top 100 m). Layer thickness increases from about 1 m at the surface to 458 m at the last level. Enhanced vertical resolution in upper layers is necessary since the seasonal mixed layer is relatively shallow and large horizontal density gradients (and vertical shear in horizontal velocities) are found near the surface.

The simulation is integrated from 1 January 1993–31 December 2022. The initial conditions, including temperature, salinity, velocity, sea surface height, sea ice concentration and sea ice thickness, are taken from the Global Ocean Reanalysis and Simulations (GLORYS2v4) produced by Mercator Ocean (Garric et al., 2017). The products used to initialize the model also provide the open boundary conditions. At the surface, the model is forced by heat, freshwater, and momentum fluxes derived from ECMWF Reanalysis v5 (ERA5) (Hersbach et al., 2020). The bulk fluxes are computed from the Coordinated Ocean-ice Reference Experiments version 2 (CORE-II) (Large & Yeager, 2009) using air temperature and specific humidity at 2 m height, shortwave and longwave radiation, total precipitation, snowfall, and wind vector at 10 m height. No temperature or salinity restoration is applied in this study. Monthly and interannually varying river discharge from Dai et al. (2009) and melting water from ice sheets and glaciers around Greenland from Bamber et al. (2018) are used as runoff. Liquid runoff is applied to the sea surface near the runoff location with an additional mixing (2×10^{-3} m^2 s^{-1}) over the top-30 m. Without runoff data after 2018, we repeat the 2017 runoff data for years 2018–2022. An iceberg module is used to calve and move Greenland icebergs as Lagrangian particles. Bamber et al. (2018) solid discharge data is used as the input. Tides are included in the model as well. The 5 day average model outputs from 1994 to 2022 are used to study the seasonal variability in Baffin Bay.

2.2. Model Evaluation

The model's ability in reproducing the hydrographic distribution, gyre circulation, and seasonal variations of local and remote forcing is examined. Primary features are well captured in our model simulation. At the sea surface (Figure S1 in Supporting Information S1), the domination of cold and fresh Arctic water and the propagation of warm and salty Atlantic water are well reproduced. Although there is a cold and salty bias in the simulated polar water. A local salinity maximum in northern Baffin Bay, likely related to brine rejection as ice forms frequently in the NOW, is also well simulated. In the vertical (Figure S2 in Supporting Information S1), the upper layer is dominated by widely spread Arctic water and the middle layer is featured by the warm Atlantic-origin water, consistent with observations. However, the boundary-interior exchange is relatively weak for the Atlantic water in the model. The basin-scale barotropic circulation (Figure S3 in Supporting Information S1), computed as an accumulation of depth-integrated volume transport from west to east at each latitude, is dominated by a cyclonic gyre. The West Greenland Current is about 3 Sv, roughly in accord with the observed transport of 3.8 Sv (Münchow et al., 2015). The southward flow in the Baffin Island Current is about 5 Sv, closely matching the observed transport of 5.1 Sv (Münchow et al., 2015). Both the spatial distribution and thickness of sea ice agree well with observations (Figure S4 in Supporting Information S1), providing a validation of simulated sea ice drift and thus surface momentum transfer. Although the simulated volume transport through straits is generally larger in magnitude (Figure S5 in Supporting Information S1), their seasonal cycles that we focus on are consistent with available observations.

3. Results

We seek to describe and understand the seasonal cycle in Baffin Bay. This is most readily accomplished by considering the dominant modes of variability in the circulation and hydrography. Seasonal variability in the circulation can be decomposed into the barotropic mode and the baroclinic mode. It will be shown that their variability is due to different forcing mechanisms and has different spatial patterns. Owing to the strong

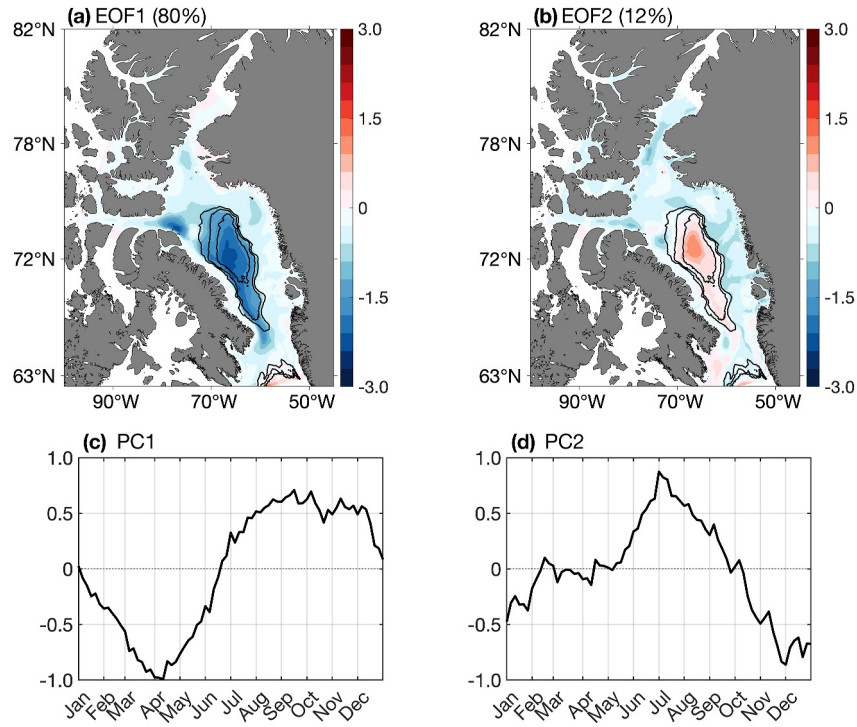

Figure 2. (a) The EOF first-mode spatial pattern (EOF1) calculated from the simulated climatological (1994–2022) 5-day averaged barotropic streamfunction in Baffin Bay and (c) its principal component (PC1) (b), (d) Same as (a) and (c) but for the second mode. The number in the bracket represents fraction of the total variance explained by each mode. The black contour lines show 1,000, 1,500, and 2,000 m isobaths.

stratification in Baffin Bay, diapycnal mixing between Atlantic and Arctic waters is weak and the seasonal cycle in the hydrography is dominated by the seasonal cycle in freshwater forcing, which is mainly by Greenland runoff and sea ice formation and melt.

3.1. Seasonal Variability of the Barotropic Circulation

We first investigate the seasonal variability of the basin-scale barotropic circulation and identify its primary forcing mechanism. Empirical orthogonal function (EOF hereafter) (Kutzbach, 1967) analysis on the 5 day mean barotropic streamfunction is carried out in Baffin Bay. Figure 2 shows the first two modes of EOF that together explain 92% of the total variance. The first mode is dominant and represents 80% of the total variance. Its spatial pattern (EOF1, Figure 2a) is a coherent mode, suggesting a recirculation gyre that spins up and down. The pattern strikingly resembles closed topographic contours with amplitude increasing from the coastal margins to the basin center. The first principal component (PC1, Figure 2c) shows a clear seasonal cycle that contributes to a weaker (stronger) cyclonic circulation (~2 Sv) in winter-spring (summer-fall). The first mode is consistent with Tang et al. (2004) that suggests stronger currents at all depths in summer and fall based on multiyear mooring observations.

We now reveal the dominant mechanism that determines the first mode. Varying winds play an important role in driving flows over closed topographic contours on time scales of a few months to years (e.g., Isachsen et al., 2003; Spall, 2016). The theory is applied successfully in the Nordic Seas and Arctic Ocean (Isachsen et al., 2003). To verify whether the first mode can be attributed to it, we first examine surface stresses ($\boldsymbol{\tau}_s$) over Baffin Bay. The $\boldsymbol{\tau}_s$ is a combination of air-ocean ($\boldsymbol{\tau}_{AO}$) and ice-ocean ($\boldsymbol{\tau}_{IO}$) stress as $\boldsymbol{\tau}_s = (1 - \mathrm{SIC})\boldsymbol{\tau}_{AO} + \mathrm{SIC}\boldsymbol{\tau}_{IO}$ where SIC is the sea ice concentration. $\boldsymbol{\tau}_{AO}$ ($\boldsymbol{\tau}_{IO}$) is computed with relative velocities between 10 m wind velocities (sea ice drift) and sea surface currents. As shown in Figure 3a, the climatological mean surface stress is mainly southeastward over Baffin Bay. A negative surface stress curl along the 1,000 m isobath appears in winter-spring compared to summer-fall (Figure 3b), which is caused by the seasonal variability in winds (sea ice) in the eastern (western)

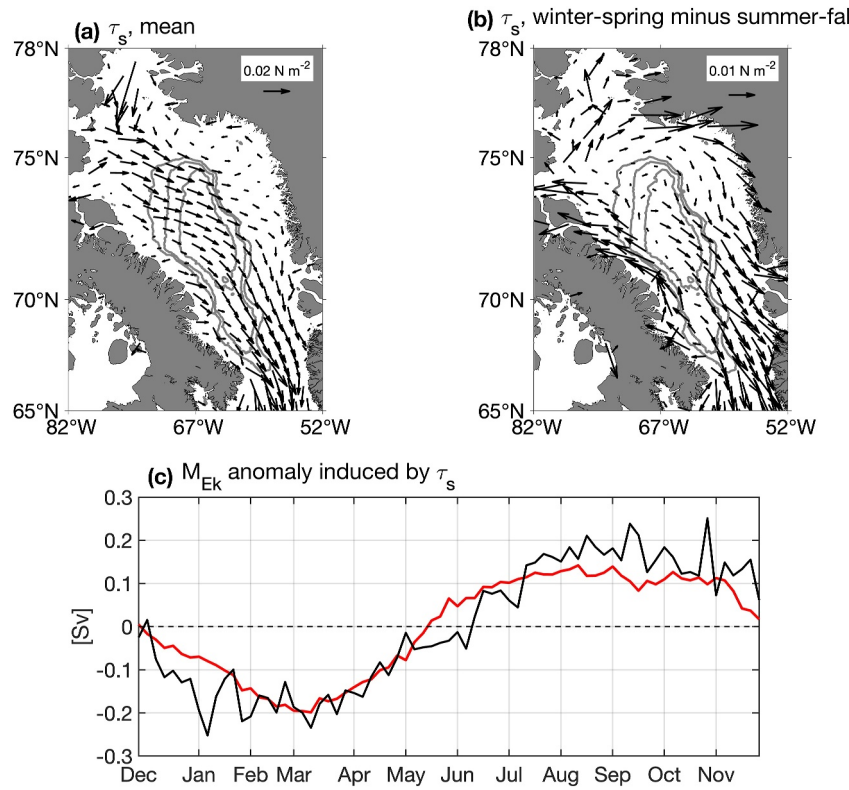

Figure 3. Simulated climatological (1994–2022) surface stress ($\boldsymbol{\tau}_s$) for (a) annual mean and (b) winter-spring (January-June) minus summer-fall (July-December). (c) Simulated climatological seasonal anomaly of the Ekman volume transport (M_{Ek}) within 1,000-m isobath induced by the surface stress curl. The surface stress is a combination of ice-ocean stress and atmosphere-ocean stress. The red line in (c) shows the PC1 (divided by five for comparison) starting from January. We note that there is about 1-month time lag between surface forcing and the ocean response. Gray contour lines in (a) and (b) show 1,000, 1,500 and 2,000 m isobaths.

Baffin Bay (Figures S6 and S7 in Supporting Information S1). The seasonality of surface stress is broadly in accord with that of the first mode (Figure 3c).

We further quantify the contribution from surface momentum forcing following a simple model developed by Spall (2023) and closely related to that of Isachsen et al. (2003). In a shallow water system with surface stresses and linear bottom drag, the depth-averaged linear momentum equation is:

$$\frac{\partial \mathbf{u}}{\partial t} + f\mathbf{k}\times\mathbf{u} = -g\nabla\eta + \frac{\boldsymbol{\tau}_s}{\rho_0 h} - \frac{C_d\mathbf{u}}{h} \tag{1}$$

where $\boldsymbol{u}$ is the depth-averaged horizontal velocity, f is the Coriolis parameter, g is the gravitational acceleration, η is the sea surface displacement, ρ_0 is the density of seawater, h is the fluid depth, C_d is the drag coefficient. Integrating Equation 1 along constant topographic contour yields:

$$\frac{\partial}{\partial t}\int_C \mathbf{u}\cdot d\mathbf{l} + \int_C f\mathbf{k}\times\mathbf{u}\cdot d\mathbf{l} = \int_C \frac{\boldsymbol{\tau}_s}{\rho_0 h}\cdot d\mathbf{l} - \int_C \frac{C_d\mathbf{u}}{h}\cdot d\mathbf{l} \tag{2}$$

where C is a topography contour, $\boldsymbol{l}$ is the along topography direction. The second term on left-hand side is proportional to the net mass flux into the enclosed region. We neglect this term since the net mass flux into the closed contour is small and acceleration by it is much smaller than the remaining terms (Spall, 2023). Then, the circulation change in the bounded region is primarily controlled by a weak imbalance between the mass convergence in the surface and bottom Ekman layers. We further assume that the surface stress along a

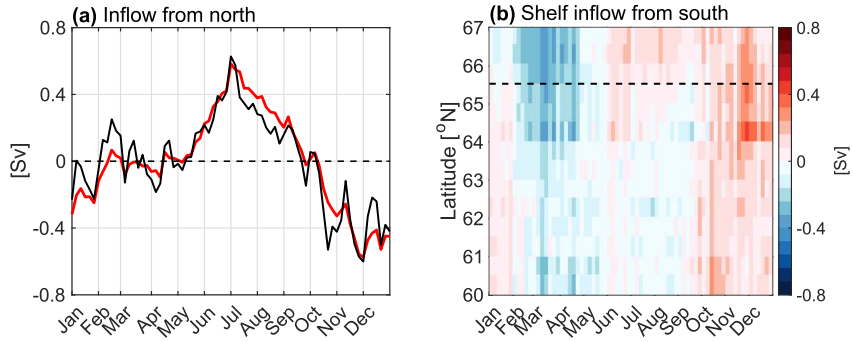

Figure 4. (a) Simulated climatological (1994–2022) seasonal anomaly of the volume transport through the northern channels. The red line shows the PC2 (divided by 1.5 for comparison). (b) Simulated climatological seasonal anomaly of the volume transport along the west Greenland shelf (shallower than 300 m) from the tip of Greenland to Davis Strait. The dashed line shows the latitude of the shallowest sill between Baffin Bay and the Labrador Sea.

topographic contour varies sinusoidally as $\boldsymbol{\tau}_s = A\sin(\omega t)$, where A is the varying amplitude and ω is the frequency. Then, the depth-averaged along-contour velocity (V) can be estimated as

$$V = \frac{A\,\sin(\omega t + \phi)}{\rho_0 C_d \left(1+\lambda^2\right)^{1/2}} \tag{3}$$

where $\lambda = \omega h/C_d$, $\phi = \tan^{-1}(-\lambda)$. According to Equation 3, the flow varies at the same frequency as the surface stress with a time lag of $-\phi/\omega$. The magnitude of flow depends on surface forcing, bottom depth and drag coefficient.

We apply the analytical solution to Baffin Bay. First, we estimate an idealized surface stress $\boldsymbol{\tau}_s$ from the Ekman volume transport within 1,000 m isobath (M_{Ek} hereafter) as $\boldsymbol{\tau}_s = M_{Ek}\rho_0 f_0/C$ where ρ_0 = 1,025 kg m^{-3}, $f_0 = 1.376 \times 10^{-4}$ s^{-1}, $C = 2.47 \times 10^6$ m is the length of 1,000 m-isobath. As shown in Figure 3c, the seasonal cycle of M_{Ek}, same as $\boldsymbol{\tau}_s$, remarkably resembles PC1 with about 1 month lead. The lead time is consistent with Equation 3, that is, 27 days, with a typical bottom drag of 4×10^{-4} m s^{-1}, a forcing period of a year, and a bottom depth of 1,000 m. The inferred amplitude of idealized surface stress is about 0.011 N m^{-2} that can result in the along 1,000 m isobath V of 2.4 cm s^{-1} according to Equation 3, qualitatively similar to 4–5 cm s^{-1} in the first mode. The latter is estimated from volume transport between 500 and 1,500 m isobath along the Baffin Island Current (~1.5 Sv within a ~35 km wide band). Barotropic responses with different values of bottom drag are shown in Table S1 in Supporting Information S1. Both amplitude and phase of V predicted by Equation 3 agree well with EOF1 and PC1, suggesting the first mode can be primarily attributed to the surface stress over Baffin Bay. We note that the coherence drops if the winds instead of the surface stress are used for prediction (Figure S8 in Supporting Information S1). This is because sea ice modifies the momentum transfer from the wind to the ocean, especially along the Baffin Island coast.

The second mode explains 12% of the total variance. The second principal component (PC2, Figure 2d) is near zero in January-April, reaches a maximum in July and a minimum in December, and in phase with total inflows from the northern channels (Figure 4a). The amplitude of the second mode along the eastern boundary is about 0.6 Sv, in good agreement with northern inflow anomalies. We note the recirculation gyre in the middle basin may be spun up by eddy momentum fluxes generated from the Baffin Island Current (Figure 2b).

The pressure anomalies associated with northern inflows propagate from north to south as a coastal wave within 5 days (time resolution of our model outputs) to induce a "synchronous" response. In addition to the northern channels, water also exchanges between Baffin Bay and outside through Davis Strait. However, the influence of the Labrador Sea is largely limited due to a shallow sill (~640 m) between Baffin Bay and the Labrador Sea. We note that the sill is located to the south of the Davis Strait observation arrays. Therefore, the seasonal cycle of transport through the Davis Strait array is largely owing to a recirculation gyre driven by the surface stress within Baffin Bay, as shown in the first mode. The inflow along the west Greenland shelf has a direct connection to lower latitudes and is anticipated to communicate outside forcing into Baffin Bay. As shown in Figure 4b, the seasonal

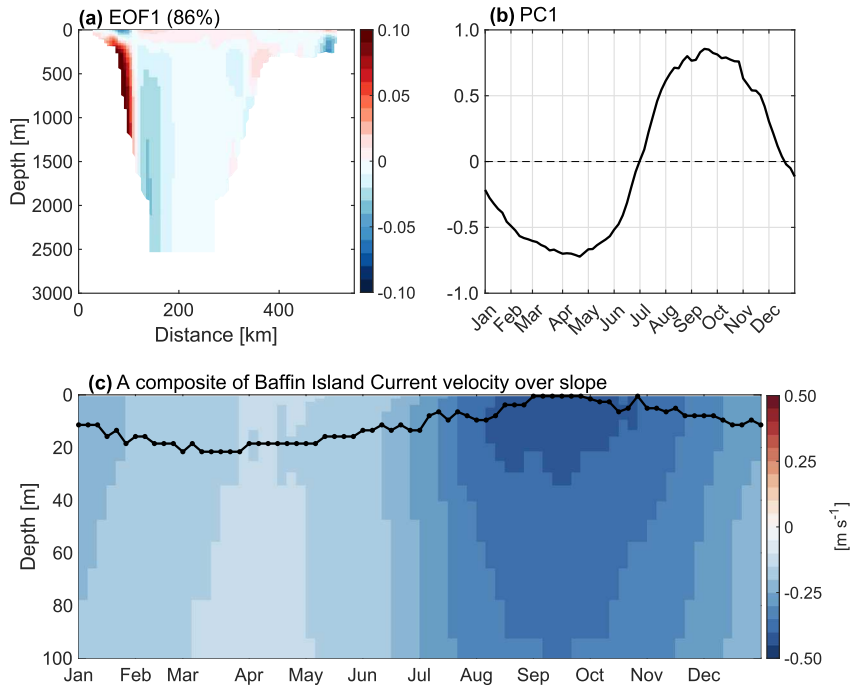

Figure 5. (a) The EOF first-mode spatial pattern (EOF1) calculated from the simulated climatological (1994–2022) 5-day averaged baroclinic cross-section velocity and (b) its principal component (PC1). The location of the section is shown in Figure 1. The baroclinic velocity is calculated as the total velocity minus the depth-averaged velocity. The number in the bracket indicates the fraction of the total variance explained by the first mode. (c) Seasonal cycle of the simulated climatological upper-100 m Baffin Island Current velocity over slope (defined positive northward). The velocity core is denoted by the black-dotted line. The velocity is composited between 71°N–73°N along the 1,000-m isobath.

variation of the shelf transport from the south is influenced by a canyon around 64°N before it enters Baffin Bay. Although the variation shows some consistency north of the canyon, the remote forcing through Davis Strait (~0.2 Sv, Figure 4b) is smaller than that from the northern channels (~0.6 Sv, Figure 4a).

3.2. Seasonal Variability of the Baroclinic Circulation

The seasonal variability in the baroclinic mode is dominated by the Baffin Island Current on the western side of the Baffin Bay, which transports liquid and solid freshwater to the Labrador Sea. The baroclinic flow accounts for more than half of the upper-600 m volume transport by the Baffin Island Current in our simulation. Lemon and Fissel (1982) finds that the Baffin Island Current exhibits a seasonal change in its baroclinicity based on 1 year mooring data. To understand the variability, we first carry out an EOF analysis on 5-day averaged baroclinic flows across a section in the middle of Baffin Bay in our simulation (denoted in Figure 1). The baroclinic flow is obtained by subtracting the depth-averaged current from the full current. The first mode explains 86% of the total variance and shows a clear seasonal cycle (Figures 5a and 5b). The spatial pattern together with the corresponding principal component contribute to an enhanced (weakened) surface intensification in the Baffin Island Current in summer-fall (winter-spring), consistent with Lemon and Fissel (1982). We note there is an onshore-offshore shift implied by EOF1 which needs more investigation in future work. We further investigate the vertical structure of the Baffin Island Current by composing its velocity along the Baffin Island slope (Figure 5c). Practically, we select sections normal to the Baffin Island Current every 0.05° between 71°N–73°N and compose current velocity along the 1,000 m isobath together. Consistent with the EOF result, the upper-100 m vertical shear of the Baffin Island Current is strong in September-October with velocity maximum at the sea surface. The current becomes more uniform in the vertical with a subsurface core in the rest of the year, especially in February-May. We note that a similar baroclinic change also occurs in the western side of Davis Strait and Smith Sound, as well as the southern side of Lancaster Sound in our simulation.

We now discuss the mechanism of this varying vertical structure. The Baffin Island Current is in geostrophic thermal wind balance (Münchow et al., 2015), which implies that a flattening of isopycnals weakens the vertical

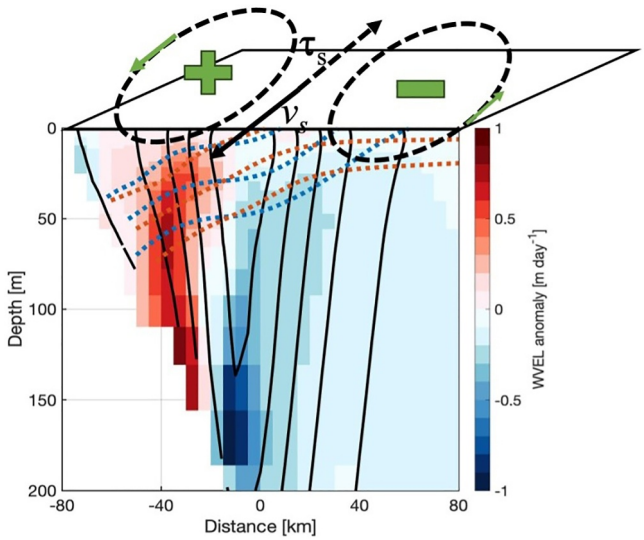

Figure 6. Simulated climatological (1994–2022) along-Baffin Island Current vertical velocity difference (shading) between winter-spring (January-June) and summer-fall (July-December). The simulated climatological southward Baffin Island Current velocity is indicated by black solid contours. The simulated climatological isopycnals are shown in blue lines for winter-spring and red lines for summer-fall. The schematic shows the mechanism of the cross-shelf circulation associated with ice-ocean stress curls. The sea surface current velocity and ice-ocean stress is denoted by $\boldsymbol{v}_s$ and $\boldsymbol{\tau}_s$, respectively. The spatially variable ice-ocean stress forms the positive (negative) surface stress curl to the west (east) of the current and thus an upwelling (downwelling) in the upper ocean.

shear of the horizontal velocity, as seen in winter-spring for the Baffin Island Current (Figure 6). Since near-surface isopycnals are flattened (tilted) in ice-covered (ice-free) seasons, we assume sea ice changes may be responsible for the isopycnal changes. As demonstrated in Leng et al. (2022), immobile thick sea ice on top of a laterally sheared slope current generates spatially uneven ice-ocean stresses and thus surface stress curl anomalies in winter-spring (schematics in Figure 6). The latter induces Ekman pumping and forms a cross-shelf circulation that flattens near-surface isopycnals. We construct a composite of the vertical velocity along the Baffin Island Current and find a cross-shelf circulation corresponding to surface stress anomalous in winter-spring (Figure 6).

We further quantify the contribution of the cross-shelf circulation to the isopycnal displacement. We assume the isopycnal displacement is smaller than its background state, that is, $\rho\,(x, y, z, t) = \overline{\rho(z)} + \rho'\,(x, y, z, t)$ with $|\rho'\,(x, y, z, t)| << |\,\overline{\rho(z)}\,|$. Then, the density change due to vertical advection is $-w\cdot\partial\overline{\rho(z)}/\partial z$. With vertical velocity of 0.65 m day^{-1} and background stratification of 0.01 kg m^{-4} at 35 m (~Ekman layer depth) on the west of the simulated Baffin Island Current, the density increase induced by the vertical advection is about 6.5×10^{-3} kg m^{-3} day^{-1}. It is close to the adiabatic density change in the simulation, which is about 6×10^{-3} kg m^{-3} day^{-1}. The adiabatic change is computed as the anomaly relative to area-mean density change in the Baffin Island Current region. The latter is diabatic and largely forced by spatially near-uniform ice-ocean freshwater flux in the region (Section 3.3). Our result suggests that the cross-shelf circulation associated with spatially uneven ice-ocean stress is largely responsible for the displacement of near-surface isopycnals and thus the change of the current baroclinicity.

3.3. Seasonal Variability of the Surface Water Mass Transformation

Baffin Bay is subjected to buoyancy forcing from the atmosphere, sea ice, and Greenland runoff. Water masses influenced by surface forcing can be quantified by the surface water mass transformation (SWMT). The SWMT in each density (σ) bin is calculated by integrating the surface density flux (B, in units of kg m^{-2} s^{-1}, defined as positive for ocean density increase) over outcrop regions (dA, in units of m^2; corresponding to σ from $\sigma - \Delta\sigma/2$ to $\sigma + \Delta\sigma/2$ where $\Delta\sigma = 0.01$ kg m^{-3}) as follows (e.g., Groeskamp et al., 2019)

$$\mathrm{SWMT}(\sigma) = \frac{1}{\Delta\sigma}\iint B dA \tag{4}$$

The density flux comprises heat and salt fluxes that are referred to as B_{heat} and B_{salt}, respectively. The heat flux is

$$B_{\mathrm{heat}} = -\frac{\alpha}{C_{\mathrm{p}}}Q \tag{5}$$

where α is the thermal expansion coefficient (in units of K^{-1}), C_{p} is the specific heat capacity of seawater (in units of J kg^{-1} K^{-1}), Q is the surface net heat flux (in units of W m^{-2}, defined as positive for ocean heat gain), which is the sum of surface non-penetrative radiation and turbulent heat fluxes at the sea surface. The salt flux is

$$B_{\mathrm{salt}} = \beta\frac{S}{1-S}(F + F^*) \tag{6}$$

where β is the haline contraction coefficient (in units of msu^{-1}, msu = kg salt/kg seawater), S is the sea surface salinity (in units of msu), F is the surface freshwater flux (in units of kg m^{-2} s^{-1}, defined as positive for ocean salinity increase), and F^* is the equivalent freshwater flux due to mass and thus the salt content exchanges (in units of kg m^{-2} s^{-1}, defined as positive/negative for ice melt/formation) (Madec & the NEMO team, 2008). We

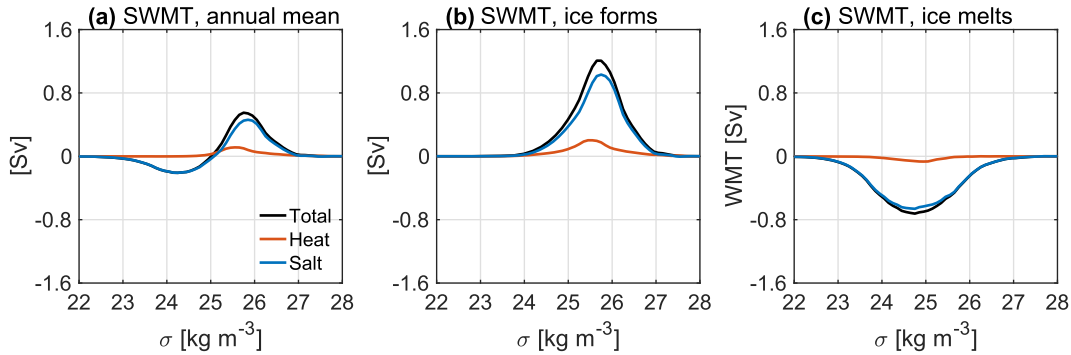

Figure 7. Simulated climatological (1994–2022) surface water mass transformation (SWMT, in units of Sv) in density space (σ, density referenced to the sea surface in units of kg m^{-3}, after subtracting 1,000 kg m^{-3}) in Baffin Bay (66.5°N–79°N, 85°W–50°W) for (a) annual mean, (b) ice formation seasons (October-April), (c) ice melting seasons (May-September). The black lines represent the total transformation. The red (blue) lines show the contribution of the surface heat (salt) flux.

note that the precipitation and evaporation in this region is much smaller (less than 1 mm day^{-1}) compared to the surface freshwater flux from sea ice melt and formation. The Greenland runoff is also applied to the sea surface. But it is promptly mixed over the top-30 m along the West Greenland shelf. Therefore, we only consider the surface ice-ocean freshwater flux, which directly forced water mass transformation in the interior of Baffin Bay, in B_{salt}.

The SWMT is calculated in the area 66.5°N–79°N, 85°W–50°W based on our simulation. It is mainly controlled by the ice-ocean freshwater flux with the effect of the surface heat flux negligible (Figure 7). The surface heat flux is smaller than 50 W m^{-2} all year round in Baffin Bay (Figures 8a and 8b). In the past 30 years, there is a net densification resulting from a net sea ice formation in the region. The latter contributes to ∼25% of the sea ice area export to the Labrador Sea via Davis Strait (Figure S9 in Supporting Information S1), broadly in accord with previous satellite-based studies (Bi et al., 2019; Kwok, 2007). The density increase is due to salinification in ice formation seasons (Figure 7b). Sea ice forms regularly in the North Water Polynya, near Nares Strait, and along the Baffin Island coast, contributing to the sea water densification (Figure 8c). The density decrease is due to freshening in ice melting seasons (Figure 7c). Sea ice melts broadly in Baffin Bay, leading to the sea water freshening (Figure 8d). We note that although net sea ice formation results in densification, we cannot conclude that Baffin Bay is overall densified. In the past 30 years, a climatological annual mean of 5.7 mSv liquid Greenland runoff is added into Baffin Bay (Figure S10 in Supporting Information S1), which is larger than the ice-ocean freshwater flux (∼−3 mSv) and thus potentially results in a net freshening in Baffin Bay. More investigation is needed to reveal how much of the Greenland runoff mixes with Baffin Bay waters in the basin interior versus getting advected out of the basin on the shelf.

4. Changes in Baffin Bay Seasonal Cycle in Recent Decades and Future

With sea ice melting and more freshwater from the Arctic and Greenland runoff, the seasonality of forcing and thus that of the ocean circulation and hydrography have changed in the past decades and are expected to be different in the future. The seasonal cycle of the barotropic circulation, controlled by the along closed-topography surface stress and volume flux from the northern channels, has not changed significantly in the past 30 years in our simulation (Figure S11 in Supporting Information S1). However, as sea ice continues to retreat in the future, we expect the seasonality to more closely follow the atmospheric forcing. More investigation is needed to understand the seasonal cycle of volume transports from the north channels and their future change. The seasonality of the baroclinicity in the Baffin Island Current has changed in the past 30 years in our simulation. The cross-shelf circulation, induced by the ice-ocean stress curl, is weakened in recent years compared to that in 1990s (Figure 9). It is because winter sea ice along Baffin Island coast becomes thinner and more mobile, which reduces the ice-ocean stresses. Continuous weakening of the cross-shelf circulation is expected, which enables the Baffin Island Current to keep its baroclinicity all year round. The seasonal cycle of the SWMT, controlled mainly by the ice-ocean freshwater flux, has also changed in the past three decades in our simulation. Although the strength of the SWMT has not changed significantly, it has shifted to lower density ranges (Figure 10) which suggests a surface

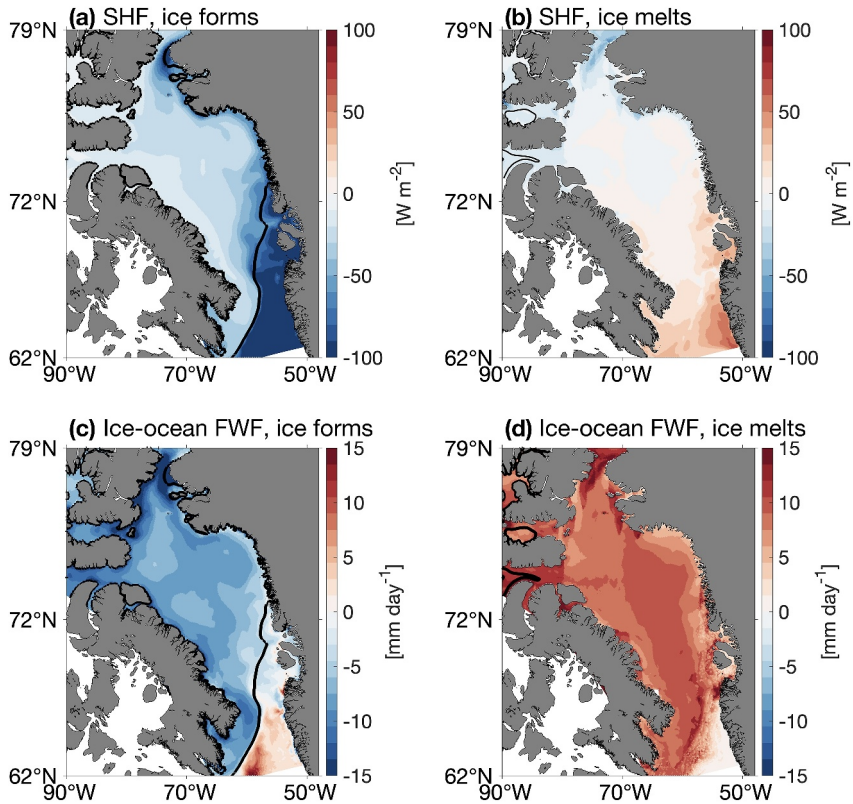

Figure 8. Simulated climatological (1994–2022) surface heat flux (SHF, positive into the ocean) in (a) ice formation seasons (October-April) and (b) ice melting seasons (May-September). (c) and (d) Same as (a) and (b) but for the ice-ocean freshwater flux (FWF, positive into the ocean). The black contours represent 70% sea ice concentration.

freshening probably due to fresher Arctic water (Zweng & Munchow, 2006) and enhanced Greenland melt (Bamber et al., 2018; Castro de la Guardia et al., 2015). Baffin Bay is expected to be freshened in the future with more freshwater coming from the Arctic and Greenland and less ice formation in the region.

5. Conclusions

Baffin Bay is a key region for connecting the Arctic Ocean and the Atlantic Ocean. The ocean circulation is important for reshaping freshwater and heat transports within the bay and exchanges between the oceans. In the mean, it is dominated by a cyclonic boundary current system: northward flowing West Greenland Current system and southward flowing Baffin Island Current system. The ocean circulation is subjected to complex forcing from

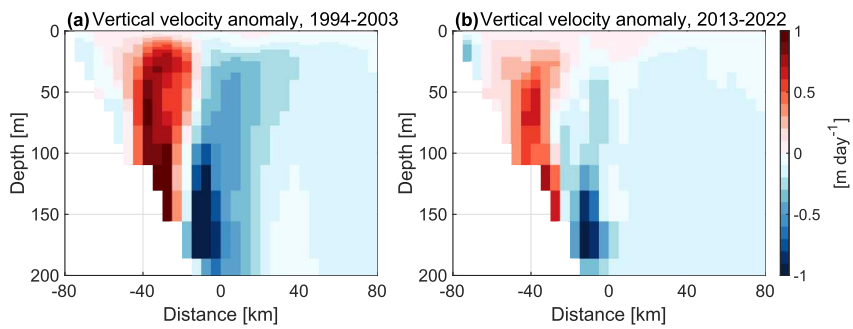

Figure 9. Simulated along-Baffin Island Current vertical velocity difference between winter-spring (January-June) and summer-fall (July-December) in (a) 1994–2003 and (b) 2013–2022. The anomalous cross-shelf circulation in winter-spring is weakened in recent years.

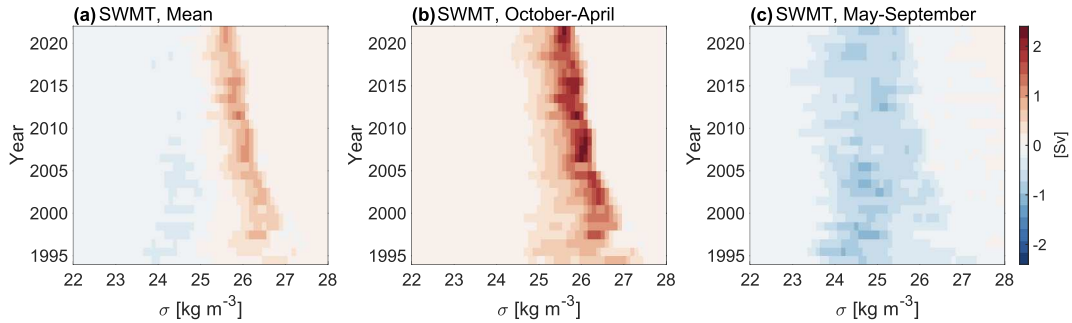

Figure 10. Evolution of the simulated surface water mass transformation (SWMT) in Baffin Bay over 1994–2022 for (a) annual mean, (b) ice formation seasons (October-April) and (c) ice melting seasons (May-September). The Baffin Bay region is defined as 66.5°N–79°N, 85°W–50°W.

the atmosphere, sea ice, Greenland and other oceans, and thus experiences significant seasonal variations. However, due to the vast sea ice cover in winter, little is known about its seasonality from direct observations.

In this study we use a regional, high-resolution coupled sea ice-ocean model to assess the seasonal cycle in the Baffin Bay ocean circulation and hydrography and investigate the mechanisms. The model reproduces the major currents, water masses and seasonally varying forcing well and thus provides confidence for our study. The barotropic circulation is generally stronger in summer and weaker in winter. The seasonality is largely controlled by the surface stress along closed isobaths. In summer-fall (July-December), the interior recirculation (∼2 Sv) spins up cyclonically with a positive surface stress curl anomaly. In winter-spring (January-June), the recirculation spins down with a negative surface stress curl anomaly. The seasonal cycle in the surface stress is due to wind anomalies in the eastern Baffin Bay and sea ice drift anomalies in the western Baffin Bay. The forcing from the north via Smith Sound and Lancaster Sound adds additional influence on the barotropic transport in the western Baffin Bay. The transport is enhanced (weakened) by ∼0.6 Sv in June-August (October-December). The influence from the Labrador Sea is smaller (∼0.2 Sv) due to two topographic effects. First, the remote forcing from the Labrador Sea is restricted by a shallow sill between Baffin Bay and the Labrador Sea. Second, the meridional coherence of variability along the west Greenland shelf is weakened by canyons that cut across the shelf south of the sill. We note that the Davis Strait observational array lies north of the shallow sill, therefore most of the seasonality in the observed volume transport is caused by a varying recirculation gyre in Baffin Bay.

The seasonality of the baroclinic circulation is dominated by the Baffin Island Current. The Baffin Island Current is surface intensified in summer-fall, while dominated by a subsurface velocity maximum in winter-spring. The seasonal variation is controlled by spatially variable ice-ocean stresses. In winter-spring, the laterally sheared southward Baffin Island Current is covered by relatively immobile sea ice. Spatially uneven northward surface stresses forms opposite surface stress curl anomalies on the western and eastern sides of the current. The anomalous curls drive a cross-shelf circulation that flattens near-surface isopycnals and thus modifies the vertical structure of the Baffin Island Current.

The water mass transformation forced by buoyancy flux from the atmosphere, sea ice, and Greenland runoff is discussed. The surface water mass transformation (SWMT) is mainly controlled by the ice-ocean freshwater flux and shows a net densification. Water masses become denser in ice formation seasons with sea ice formation near Nares Strait, in the North Water Polynya, and along the Baffin Island coast. The waters are freshened in ice melting seasons with broad sea ice melt in Baffin Bay. The sea ice formation exceeds its melting and contributes to ∼25% of the sea ice export through Davis Strait. Plenty of liquid freshwater is provided by Greenland runoff to the west Greenland shelf (∼5.7 mSv), which exceeds the amount of ice-ocean freshwater flux (∼−3 mSv). However, more investigation is needed to quantify the contribution of Greenland runoff to water mass transformation within Baffin Bay.

The seasonal cycle in Baffin Bay has shown some changes in the past 30 years with sea ice melting and more freshwater from the Arctic and Greenland. In a warming climate, a more atmospheric driven barotropic recirculation gyre, a year-round baroclinic Baffin Island Current and a fresher Baffin Bay are expected.

Although our simulation enables a more complete understanding of Baffin Bay ocean circulation and hydrography that complements what is known from summer observations, the study still has some limitations. The horizontal resolution (~4 km) in our model is not adequate to fully resolve eddies, which leads to a weaker zonally mixed Atlantic water compared to observations (Figure S2 in Supporting Information S1, Münchow et al., 2015). A higher horizontal resolution is also crucial for fjord processes that are important for Greenland ice melting and advection on the shelf. Therefore, models with enhanced resolution and more observations are needed to better validate and understand the processes in Baffin Bay.

Data Availability Statement

All data used in the figures are available at https://doi.org/10.5281/zenodo.13731084 (Shan et al., 2024). The model code based on the NEMO model is available at https://www.nemo-ocean.eu/. Details on the ANHA configuration are available at https://canadian-nemo-ocean-modelling-forum-commuity-of-practice.readthedocs.io/en/latest/Institutions/UofA/Configurations/ANHA12/index.html. Model outputs and files for the experiment used in this paper are available upon request. Observational datasets used to validate model results are available as follows. Sea surface temperature from ERSSTv5 is available at https://psl.noaa.gov/data/gridded/data.noaa.ersst.v5.html. Sea surface salinity from SMOS can be download from https://data.marine.copernicus.eu/viewer/expert?view=dataset&dataset=MULTIOBS_GLO_PHY_SSS_L4_MY_015_015. Sea ice thickness from the CryoSat-2 satellite is available at https://catalogue.ceda.ac.uk/uuid/45b5b1e556da448089e2b57452f277f5. Temperature and salinity for the Arctic Ocean from UDASH can be downloaded from https://doi.pangaea.de/10.1594/PANGAEA.872931. Data are processed and analyzed using MATLAB R2022b (MathWorks, 2022).

Acknowledgments
This work was supported by National Science Foundation Grant (OPP-2211691) to MAS, the Natural Sciences and Engineering Research Council of Canada Grants (rgpin 227438-09 and rgpin 2020-04344) to PGM, and Ocean University of China Fellowship for International Postdoctoral Research to XS. The numerical model was run on infrastructure, and using an annual allocation of resources, provided by the Digital Research Alliance of Canada to PGM. We thank two anonymous reviewers for providing constructive feedback on the manuscript.

References

Addison, V. G. (1987). Physical oceanography of the northern Baffin bay – Nares Strait region. Master's thesis. 110pp.

Bamber, J. L., Tedstone, A. J., King, M. D., Howat, I. M., Enderlin, E. M., van den Broeke, M. R., & Noel, B. (2018). Land ice freshwater budget of the arctic and north atlantic oceans: 1. Data, methods, and results. *Journal of Geophysical Research: Oceans*, *123*(3), 1827–1837. https://doi.org/10.1002/2017JC013605

Bi, H., Zhang, Z., Wang, Y., Xu, X., Liang, Y., Huang, J., et al. (2019). Baffin bay sea ice inflow and outflow: 1978–1979 to 2016–2017. *The Cryosphere*, *13*(3), 1025–1042. https://doi.org/10.5194/tc-13-1025-2019

Bourke, R. H., Addison, V. G., & Paquette, R. G. (1989). Oceanography of Nares Strait and northern Baffin-Bay in 1986 with emphasis on deep and bottom water formation. *Journal of Geophysical Research*, *94*(C6), 8289–8302. https://doi.org/10.1029/JC094iC06p08289

Castro de la Guardia, L., Hu, X., & Myers, P. G. (2015). Potential positive feedback between Greenland Ice Sheet melt and Baffin Bay heat content on the west Greenland shelf. *Geophysical Research Letters*, *42*(12), 4922–4930. https://doi.org/10.1002/2015GL064626

Curry, B., Lee, C. M., Petrie, B., Moritz, R. E., & Kwok, R. (2014). Multiyear volume, liquid freshwater, and sea ice transports through Davis Strait, 2004–10. *Journal of Physical Oceanography*, *44*(4), 1244–1266. https://doi.org/10.1175/JPO-D-13-0177.1

Dai, A., Qian, T., Trenberth, K. E., & Milliman, J. D. (2009). Changes in continental freshwater discharge from 1948 to 2004. *Journal of Climate*, *22*(10), 2773–2792. https://doi.org/10.1175/2008JCLI2592.1

Fichefet, T., & Maqueda, M. A. M. (1997). Sensitivity of a global sea ice model to the treatment of ice thermodynamics and dynamics. *Journal of Geophysical Research*, *102*(C6), 12609–12646. https://doi.org/10.1029/97JC00480

Fissel, D. B., Lemon, D. D., & Birch, J. R. (1982). Major features of the summer near-surface circulation of western Baffin Bay, 1978 and 1979. *Arctic*, *35*(1), 180–200. https://doi.org/10.14430/arctic2318

Garric, G., Parent, L., Greiner, E., Drévillon, M., Hamon, M., Lellouche, J. M., et al. (2017). *Performance and quality assessment of the global ocean eddy-permitting physical reanalysis GLORYS2V4*. EGU General Assembly. Paper presented at.

Goosse, H., & Fichefet, T. (1999). Importance of ice-ocean interactions for the Global Ocean circulation: A model study. *Journal of Geophysical Research*, *104*(C10), 23337–23355. https://doi.org/10.1029/1999JC900215

Grivault, N., Hu, X., & Myers, P. G. (2017). Evolution of Baffin Bay water masses and transports in a numerical sensitivity experiment under enhanced Greenland melt. *Atmosphere-Ocean*, *55*(3), 169–194. https://doi.org/10.1080/07055900.2017.1333950

Groeskamp, S., Griffies, S. M., Iudicone, D., Marsh, R., Nurser, A. J. G., & Zika, J. D. (2019). The water mass transformation framework for ocean physics and biogeochemistry. *Annual Review of Marine Science*, *11*(1), 271–305. https://doi.org/10.1146/annurev-marine-010318-095421

Haine, T. W. N., Curry, B., Gerdes, R., Hansen, E., Karcher, M., Lee, C., et al. (2015). Arctic freshwater export: Status, mechanisms, and prospects. *Global and Planetary Change*, *125*, 13–35. https://doi.org/10.1016/j.gloplacha.2014.11.013

Hersbach, H., Bell, B., Berrisford, P., Hirahara, S., Horányi, A., Muñoz-Sabater, J., et al. (2020). The ERA5 global reanalysis. *Quarterly Journal of the Royal Meteorological Society*, *146*(730), 1999–2049. https://doi.org/10.1002/qj.3803

Hu, X., Sun, J., Chan, T. O., & Myers, P. G. (2018). Thermodynamic and dynamic ice thickness contributions in the Canadian Arctic Archipelago in NEMO-LIM2 numerical simulations. *The Cryosphere*, *12*(4), 1233–1247. https://doi.org/10.5194/tc-12-1233-2018

Ingram, R. G., Bacle, J., Barber, D. G., Gratton, Y., & Melling, H. (2002). An overview of physical processes in the North Water. *Deep-Sea Research II*, *49*(22–23), 4893–4906. https://doi.org/10.1016/S0967-0645(02)00169-8

Isachsen, P. E., LaCasce, J. H., Mauritzen, C., & Häkkinen, S. (2003). Wind-driven variability of the large-scale recirculating flow in the nordic seas and Arctic Ocean. *Journal of Physical Oceanography*, *33*(12), 2534–2550. https://doi.org/10.1175/1520-0485(2003)033<2534:WVOTLR>2.0.CO;2

Kutzbach, J. E. (1967). Empirical eigenvectors of sea-level pressure, surface temperature and precipitation complexes over North America. *Journal of Applied Meteorology and Climatology*, *6*(5), 791–802. https://doi.org/10.1175/1520-0450(1967)006<0791:EEOSLP>2.0.CO;2

Kwok, R. (2007). Baffin bay ice drift and export: 2002–2007. *Geophysical Research Letters*, *34*(19), L1950. https://doi.org/10.1029/2007GL031204

Landy, J. C., Ehn, J. K., Babb, D. G., Thériault, N., & Barber, D. G. (2017). Sea ice thickness in the eastern Canadian arctic: Hudson bay complex and Baffin bay. *Remote Sensing of Environment*, *200*, 281–294. https://doi.org/10.1016/j.rse.2017.08.019

Large, W. G., & Yeager, S. G. (2009). The global climatology of an interannually varying air–sea flux data set. *Climate Dynamics*, *33*(2–3), 341–364. https://doi.org/10.1007/s00382-008-0441-3

Lemon, D. D., & Fissel, D. B. (1982). Seasonal variations in currents and water properties in Northwestern Baffin Bay, 1978-1979. *Arctic*, *35*(1), 211–218. https://doi.org/10.14430/arctic2320

Leng, H., Spall, M. A., & Bai, X. (2022). Temporal evolution of a geostrophic current under sea ice: Analytical and numerical solutions. *Journal of Physical Oceanography*, *52*(6), 1191–1204. https://doi.org/10.1175/JPO-D-21-0242.1

Madec, G., & the NEMO team. (2008). *NEMO ocean engine*. Institut Pierre-Simon Laplace (IPSL).

MathWorks. (2022). MATLAB r2022b. [Software]. Retrieved from https://www.mathworks.com/products/new_products/release2022b.html. accessed 06 June 2024.

Melling, H., Agnew, T. A., Falkner, K. K., Greenberg, D. A., Lee, C. M., Münchow, A., et al. (2008). Fresh-water fluxes via pacific and arctic outflows across the Canadian polar shelf. In R. R. Dickson, J. Meincke, & P. Rhines (Eds.), *Arctic-subarctic ocean fluxes* (pp. 193–247). Springer.

Melling, H., Gratton, Y., & Ingram, G. (2001). Ocean circulation within the North water polynya of Baffin bay. *Atmosphere-Ocean*, *39*(3), 301–325. https://doi.org/10.1080/07055900.2001.9649683

Muench, R. (1971). The physical oceanography of the northern Baffin Bay region. Report No. 1. *Technical Report*. Baffin Bay - North Water Scientific.

Münchow, A. (2016). Volume and freshwater flux observations from Nares Strait to the west of Greenland at daily time scales from 2003 to 2009. *Journal of Physical Oceanography*, *46*(1), 141–157. https://doi.org/10.1175/JPO-D-15-0093.1

Münchow, A., Falkner, K. K., & Melling, H. (2015). Baffin Island and west Greenland current systems in northern Baffin bay. *Progress in Oceanography*, *132*, 305–317. https://doi.org/10.1016/j.pocean.2014.04.001

Peterson, I., Hamilton, J., Prinsenberg, S., & Pettipas, R. (2012). Wind-forcing of volume transport through lancaster Sound. *Journal of Geophysical Research*, *117*(C11), C11018. https://doi.org/10.1029/2012JC008140

Rudels, B. (2011). Volume and freshwater transports through the Canadian arctic archipelago–baffin bay system. *Journal of Geophysical Research*, *116*, C00D10. https://doi.org/10.1029/2011JC007019

Shan, X., Spall, M., Pennelly, C., & Myers, P. (2024). Seasonal variability in Baffin bay. [Dataset]. https://doi.org/10.5281/zenodo.13731084

Spall, M. A. (2016). Wind-driven flow over topography. *Journal of Marine Research*, *74*(4), 229–248. https://doi.org/10.1357/002224016820870657

Spall, M. A. (2023). Wind-forced seasonal exchange between marginal seas and the open ocean. *Journal of Physical Oceanography*, *53*(3), 763–777. https://doi.org/10.1175/JPO-D-22-0151.1

Tang, C. C. L., Ross, C. K., Yao, T., Petrie, B., DeTracey, B. M., & Dunlap, E. (2004). The circulation, water masses and sea-ice of Baffin Bay. *Progress in Oceanography*, *63*(4), 183–228. https://doi.org/10.1016/j.pocean.2004.09.005

Wang, Q., Shu, Q., Wang, S., Beszczynska-Moeller, A., Danilov, S., de Steur, L., et al. (2023). A review of arctic–subarctic ocean linkages: Past changes, mechanisms, and future projections. *Ocean-Land-Atmosphere Research*, *2*, 0013. https://doi.org/10.34133/olar.0013

Yao, T., & Tang, C. L. (2003). The formation and maintenance of the North water polynya. *Atmosphere-Ocean*, *41*(3), 187–201. https://doi.org/10.3137/ao.410301

Zhang, J., Weijer, W., Steele, M., Cheng, W., Verma, T., & Veneziani, M. (2021). Labrador Sea freshening linked to Beaufort Gyre freshwater release. *Nature Communications*, *12*(1), 1229. https://doi.org/10.1038/s41467-021-21470-3

Zweng, M. M., & Munchow, A. (2006). Warming and freshening of Baffin bay, 1916–2003. *Journal of Geophysical Research*, *111*(C7), C07016. https://doi.org/10.1029/2005JC003093

References From the Supporting Information

Behrendt, A., Sumata, H., Rabe, B., & Schauer, U. (2018). Udash – Unified database for arctic and subarctic hydrography. *Earth System Science Data*, *10*(2), 1119–1138. https://doi.org/10.5194/essd-10-1119-2018

Hendricks, S., Paul, S., & Rinne, E. (2024). ESA Sea Ice Climate Change Initiative (Sea_Ice_cci): Northern hemisphere sea ice thickness from the CryoSat-2 satellite on a monthly grid (L3C), v3.0. In *NERC EDS centre for environmental data analysis*. Retrieved from https://catalogue.ceda.ac.uk/uuid/45b5b1e556da448089e2b57452f277f5

Huang, B., Thorne, P. W., Banzon, V. F., Boyer, T., Chepurin, G., Lawrimore, J. H., et al. (2017). Extended reconstructed sea surface temperature, version 5 (ERSSTv5): Upgrades, validations, and intercomparisons. *Journal of Climate*, *30*(20), 8179–8205. https://doi.org/10.1175/JCLI-D-16-0836.1

Nicolas, K., Michel, H., Jacqueline, B., Jean-Luc, V., Gilles, R., Alexandre, S., & Nicolas, R. (2021). Objective analysis of SMOS and SMAP Sea Surface Salinity to reduce large scale and time dependent biases from low to high latitudes. *Journal of Atmospheric and Oceanic Technology*, *38*(3), 405–421. https://doi.org/10.1175/JTECH-D-20-0093.1